

# Coupling of Two Ethyne Molecules at Rhodium versus Coupling of Two Rhodium Atoms at Ethyne. 1. Electronic Control on the Interconversion of ( $\mu$ - $\eta^2$ , $\eta^2$ -Ethyne)- and ( $\mu$ - $\eta^1$ , $\eta^1$ -Ethyne)dirhodium Complexes

Claudio Bianchini,\* Dante Masi, Andrea Meli, Maurizio Peruzzini, and Alberto Vacca

*Istituto per lo Studio della Stereochimica ed Energetica dei Composti di Coordinazione, CNR, Via J. Nardi 39, 50132 Firenze, Italy*

Franco Laschi and Piero Zanello

*Dipartimento di Chimica, Università di Siena, Via Pian dei Mantellini 44, 53100 Siena, Italy*

Received May 16, 1990

Depending on the metal to ethyne ratio, the reaction of [(triphos)RhCl(C<sub>2</sub>H<sub>4</sub>)] (1; triphos = MeC(CH<sub>2</sub>PPh<sub>2</sub>)<sub>3</sub>) with ethyne forms either the binuclear complex [(triphos)Rh( $\mu$ -Cl)( $\mu$ - $\eta^2$ , $\eta^2$ -C<sub>2</sub>H<sub>2</sub>)Rh(triphos)]Cl (2) or the mononuclear rhodacyclopentadiene complex [(triphos)RhCl( $\eta^2$ -C<sub>4</sub>H<sub>4</sub>)] (3). The crystal structure of the complex cation [(triphos)Rh( $\mu$ -Cl)( $\mu$ - $\eta^2$ , $\eta^2$ -C<sub>2</sub>H<sub>2</sub>)Rh(triphos)]<sup>+</sup> (2<sup>+</sup>) has been determined by X-ray methods. In the structure, a chloride ligand and an ethyne molecule bridge two (triphos)Rh fragments with a Rh-Rh separation (3.306 (2) Å) that corresponds to no formal metal-metal bond. The ethyne molecule is positioned in the  $\mu$ - $\eta^2$ , $\eta^2$  mode and formally serves as a four-electron donor (C-C bond length of 1.36 (2) Å). The cation 2<sup>+</sup> is highly fluxional in solution on the NMR time scale. The fluxional process involves two distinct mechanisms. Complex 2<sup>+</sup> undergoes single-stepped two-electron oxidation by chemical or electrochemical methods, converting to the  $\mu$ - $\eta^1$ , $\eta^1$  derivative [(triphos)Rh( $\mu$ -Cl)<sub>2</sub>( $\mu$ - $\eta^1$ , $\eta^1$ -C<sub>2</sub>H<sub>2</sub>)Rh(triphos)]<sup>2+</sup> (5<sup>2+</sup>), where ethyne bridges the two metals as a cis-dimetalated olefin. The reaction is reversible. Complex 2<sup>+</sup> is regenerated by two one-electron-reduction steps from 5<sup>2+</sup>. Controlled-potential macroelectrolysis at the potential of the first reduction step allows one to generate the paramagnetic species [(triphos)Rh( $\mu$ -Cl)<sub>2</sub>( $\mu$ - $\eta^1$ , $\eta^1$ -C<sub>2</sub>H<sub>2</sub>)Rh(triphos)]<sup>+</sup> (5<sup>+</sup>), which has been characterized by X-band ESR spectroscopy. In the absence of external ligands, the cation 2<sup>+</sup> undergoes two-electron oxidation, forming the  $\mu$ -OH derivative [(triphos)Rh( $\mu$ -Cl)( $\mu$ -OH)( $\mu$ - $\eta^1$ , $\eta^1$ -C<sub>2</sub>H<sub>2</sub>)Rh(triphos)]<sup>2+</sup> (4<sup>2+</sup>) through abstraction of a hydroxy group from adventitious water in solution. From preliminary X-ray analysis and detailed spectroscopic studies it is concluded that 5<sup>2+</sup> and 4<sup>2+</sup> share the same cis-dimetalated bonding mode of the ethyne bridge. Complex 4<sup>2+</sup> transforms into 5<sup>2+</sup> by reaction with gaseous HCl while water is eliminated. The reaction of the perchlorate salt of 4<sup>2+</sup> with CF<sub>3</sub>COOH yields H<sub>2</sub>O and the  $\mu$ -carboxylate complex [(triphos)Rh( $\mu$ -O<sub>2</sub>CCF<sub>3</sub>)( $\mu$ -Cl)( $\mu$ - $\eta^1$ , $\eta^1$ -C<sub>2</sub>H<sub>2</sub>)Rh(triphos)](ClO<sub>4</sub>)<sub>2</sub> (6). With the exception of the paramagnetic species 5<sup>+</sup>, all of the complexes have been isolated in the solid state as ClO<sub>4</sub><sup>-</sup>, PF<sub>6</sub><sup>-</sup>, and/or BPh<sub>4</sub><sup>-</sup> salts. The redox properties of the relevant compounds in CH<sub>2</sub>Cl<sub>2</sub> have been studied by electrochemical techniques. This has allowed us to shed some light on the mechanistic aspects of the chemically reversible pathway connected to the interconversion 2<sup>+</sup>/5<sup>2+</sup>. In particular, we show that the oxidation of 2<sup>+</sup> to 5<sup>2+</sup> most likely occurs via an EC<sub>a</sub>C<sub>a</sub>E mechanism, where E = electron transfer, C<sub>a</sub> = addition of chloride, and C<sub>r</sub> = stereochemical rearrangement of the ethyne bridge.

## Introduction

Surveying the reactions of ethyne with transition-metal complexes, one is first struck by the myriad of organometallic complexes and organic compounds that may be produced.<sup>1</sup> Then, one readily infers that the first step of any stoichiometric or catalytic reaction between a metal complex and ethyne almost invariably involves the coordination of an ethyne molecule to the metal.<sup>2</sup> What

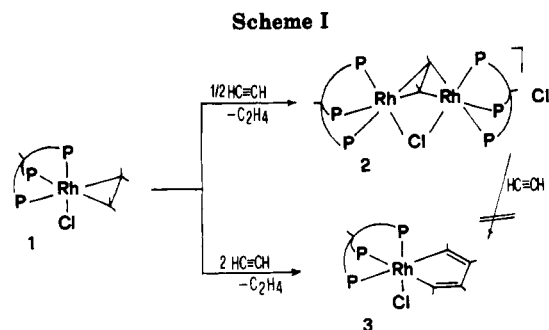
happens afterwards is a matter that depends on many factors, including the nature of the metal fragment, the stoichiometry, the temperature, the pressure, etc. As a consequence, any rigorous and reliable study on the interaction of ethyne with a certain metal fragment necessarily requires a careful control of parameters.

In the present work, we describe the products obtained by the reaction of the complex [(triphos)RhCl(C<sub>2</sub>H<sub>4</sub>)]<sup>3</sup> (1) with ethyne (triphos = MeC(CH<sub>2</sub>PPh<sub>2</sub>)<sub>3</sub>). By a judicious selection of the reaction conditions, we have been able to isolate either the product formed by coupling two metals through ethyne, [(triphos)Rh( $\mu$ -Cl)( $\mu$ - $\eta^2$ , $\eta^2$ -C<sub>2</sub>H<sub>2</sub>)Rh(triphos)]Cl (2), or the product resulting from coupling two ethyne molecules at the metal, [(triphos)RhCl( $\eta^2$ -C<sub>4</sub>H<sub>4</sub>)] (3). Complex 2 belongs to the widespread family of bridging-alkyne dimers.<sup>4</sup> These have been extensively

(1) (a) Wegner, G. *Angew. Chem., Int. Ed. Engl.* 1981, 20, 361. (b) Reppe, W.; van Kutepow, N.; Magin, A. *Angew. Chem., Int. Ed. Engl.* 1969, 8, 727. (c) Mouljin, J. A.; Reitsma, H. J.; Boelhouwer, C. J. *Catal.* 1972, 25, 434. (d) Thompson, J. S.; Whitney, J. F. *J. Am. Chem. Soc.* 1983, 105, 5488. (e) Kamata, M.; Hirotsu, K.; Higuchi, T.; Kido, M.; Tatsumi, K.; Yoshida, T.; Otsuka, S. *Inorg. Chem.* 1983, 22, 2416. (f) Alt, H.; Eichner, M. E.; Jansen, B. M. *Angew. Chem., Int. Ed. Engl.* 1982, 21, 861. (g) Thomas, J. L. *Inorg. Chem.* 1978, 17, 1507. (h) Pörschke, K. R. *J. Am. Chem. Soc.* 1989, 111, 5691. (i) Staal, L. H.; van Koten, G.; Vrieze, K.; Ploeger, F.; Stam, C. H. *Inorg. Chem.* 1981, 20, 1830. (j) Bonnet, J. J.; Mathieu, R. *Inorg. Chem.* 1978, 17, 1973. (k) Bailey, W. L.; Chisholm, M. H.; Cotton, F. A.; Rankel, L. A. *J. Am. Chem. Soc.* 1978, 100, 5764. (l) Wang, Y.; Coppens, P. *Inorg. Chem.* 1976, 15, 1122. (m) Lourdichi, M.; Mathieu, R. *Organometallics* 1986, 5, 2067. (n) Alt, H. G.; Engelhardt, H. E.; Rausch, M. D.; Kool, L. *J. Organomet. Chem.* 1987, 329, 61. (o) Yamazaki, H.; Wakatsuki, Y. *J. Organomet. Chem.* 1984, 272, 251.

(2) (a) Chausser, M. G.; Rodionov, Yu. M.; Misin, V. M.; Cherkashin, M. I. *Russ. Chem. Rev. (Engl. Transl.)* 1989, 1264. (b) Maitlis, P. M. *Acc. Chem. Res.* 1976, 9, 93. (c) Bruck, M. A.; Copenhaver, A. S.; Wigley, D. E. *J. Am. Chem. Soc.* 1987, 109, 6525. (d) Strickler, J. R.; Wexler, P. A.; Wigley, D. E. *Organometallics* 1988, 7, 2067.

(3) Bianchini, C.; Meli, A.; Peruzzini, M.; Vizza, F.; Frediani, P.; Ramirez, J. A. *Organometallics* 1990, 9, 226.



studied because of their relevance to several fields of both fundamental and applied organometallic chemistry, particularly heterogeneous catalysis. We report here a chemical and electrochemical study on the connections between the overall electron number of the (ethyne)dirrhodium complex and the bonding mode of the  $\text{C}_2\text{H}_2$  moiety.

The rhodacyclopentadiene complex **3** promotes a number of stoichiometric and catalytic functionalization reactions of ethyne, which will be described in the following article along with a full characterization of the complex.

### Results and Discussion

#### Reaction of [(triphos)RhCl( $\text{C}_2\text{H}_4$ )] with Ethyne.

Depending on the metal to ethyne ratio, the reaction of [(triphos)RhCl( $\text{C}_2\text{H}_4$ )] (**1**) with ethyne forms either brick red crystals of [(triphos)Rh( $\mu\text{-Cl}$ )( $\mu\text{-}\eta^2,\eta^2\text{-C}_2\text{H}_2$ )Rh(triphos)]Cl (**2**) or off-white crystals of [(triphos)RhCl( $\eta^2\text{-C}_4\text{H}_4$ )] (**3**) (Scheme I). In both cases, ethylene is evolved. The reactions can be monitored by  $^{31}\text{P}\{\text{H}\}$  NMR spectroscopy, as the two compounds exhibit readily distinguishable sets of resonances. In a typical experiment,  $\text{C}_2\text{H}_2$  is syringed into an NMR tube containing a solution of **1** in THF- $d_6$  (THF = tetrahydrofuran),  $\text{CD}_2\text{Cl}_2$ , or  $(\text{CD}_3)_2\text{CO}$  at room temperature. On addition of a stoichiometric amount of ethyne, a slow reaction takes place, which produces the dimer **2** with no trace of the rhodacyclopentadiene complex **3**. Trebling the amount of  $\text{C}_2\text{H}_2$  increases the conversion of **1** into **2** while **3** begins to form. The last complex becomes the predominant product for larger excesses of ethyne and is the only product when  $\text{C}_2\text{H}_2$ -saturated solvents are used at  $0^\circ\text{C}$ . In view of the NMR evidence, efficient, large-scale preparations for **2** and **3** have been designed. These imply a strict control on the temperature, as it affects both the rate of the reactions and the concentration of ethyne in solution. In particular, the dimer **2** can be quantitatively obtained by bubbling ethyne into refluxing solutions of **1** in THF for 5 min, whereas the rhodacyclopentadiene complex is synthesized by dissolving **1** in cold  $\text{C}_2\text{H}_2$ -saturated dichloromethane. Complex **2** does not transform into **3** by treatment with an excess of ethyne.

**Characterization of the ( $\mu\text{-}\eta^2,\eta^2\text{-Ethyne}$ )dirrhodium Complex **2**.** Complex **2** is air-stable in the solid state and in solution, where it behaves as a 1:1 electrolyte. Crystals

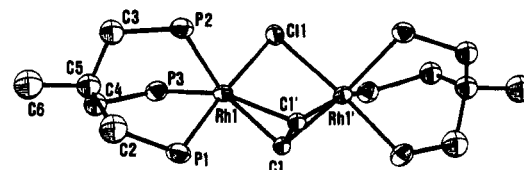


**Figure 1.** ORTEP drawing of the complex cation [(triphos)Rh( $\mu\text{-Cl}$ )( $\mu\text{-}\eta^2,\eta^2\text{-C}_2\text{H}_2$ )Rh(triphos)] $^{2+}$  (**2<sup>+</sup>**). All of the hydrogen atoms and phenyl rings of triphos are omitted for clarity.

**Table I.** Selected Bond Distances (Å) and Angles (deg) for **2c**•DMF

Rh1-P1	2.238 (5)	P3-C4	1.82 (2)
Rh1-P2	2.369 (5)	C1-C1'	1.36 (2)
Rh1-P3	2.377 (5)	C2-C5	1.60 (3)
Rh1-Cl1	2.449 (4)	C3-C5	1.53 (3)
Rh1-C1	2.13 (2)	C4-C5	1.56 (2)
Rh1-C1'	2.14 (2)	C5-C6	1.57 (3)
P1-C2	1.83 (2)	Rh1...Rh1'	3.306 (2)
P2-C3	1.83 (2)		
P1-Rh1-P2	87.3 (2)	P2-Rh1-Cl1	95.1 (1)
P1-Rh1-P3	89.1 (2)	P3-Rh1-Cl1	94.0 (1)
P2-Rh1-P3	90.7 (2)	P1-C2-C5	116 (1)
P1-Rh1-C1	93.1 (4)	P2-C3-C5	118 (1)
P2-Rh1-C1	154.6 (4)	P3-C4-C5	114 (1)
P2-Rh1-C1'	117.4 (4)	C2-C5-C3	108 (1)
P3-Rh1-C1	114.7 (4)	C2-C5-C4	110 (1)
P3-Rh1-C1'	151.8 (4)	C3-C5-C4	116 (1)
Rh1-P1-C2	111.9 (6)	C3-C5-C6	108 (1)
Rh1-P2-C3	108.2 (6)	C4-C5-C6	109 (1)
Rh1-P3-C4	111.2 (6)	Rh1-Cl1-Rh1'	84.9 (2)
P1-Rh1-Cl1	176.0 (1)		

suitable for X-ray diffraction study were obtained as the dimethylformamide (DMF) solvate of the metathesis product [(triphos)Rh( $\mu\text{-Cl}$ )( $\mu\text{-}\eta^2,\eta^2\text{-C}_2\text{H}_2$ )Rh(triphos)]BPh $_4$  (**2c**). This compound can be readily prepared by reacting **2** with 1 equivalent of NaBPh $_4$  (Scheme II). The structure of the complex cation as determined by X-ray analysis is shown in Figure 1. Selected bond lengths and angles are given in Table I. The complex has  $C_{2v}$  symmetry; indeed, the dinuclear unit is built from a mononuclear unit by the binary crystallographic symmetry. In the structure, a chloride ligand and an ethyne molecule bridge two (triphos)Rh fragments with a Rh-Rh separation of 3.306 (2) Å. This corresponds to no formal metal-metal bond and can be contrasted with typical Rh-Rh separations in "perpendicular"  $\mu$ -acetylene complexes where a metal-metal bond is present (2.644–2.740 Å).<sup>5</sup> The coordination geometry about each Rh is distorted-octahedral or trigonal-bipyramidal if the alkyne is assumed to occupy a single coordination site of each metal. The ethyne molecule is positioned in the  $\mu\text{-}\eta^2,\eta^2$  mode and formally serves as a four-electron donor for the two rhodium centers. This is confirmed by several spectroscopic data (see below), including the IR spectrum, which contains  $\nu(\text{C}\equiv\text{C})$  at  $1320\text{ cm}^{-1}$ . The alkyne C-C bond length of 1.36 (2) Å is longer than those found in free ethyne (1.204 Å)<sup>6</sup> and ethylene (1.337 (3) Å)<sup>7</sup> and is comparable with those in  $[\text{Mo}_2(\text{O}-i\text{-Pr})_4(\text{py})_2(\mu\text{-O}-i\text{-Pr})_2(\mu\text{-C}_2\text{H}_2)]$  (1.368 (6) Å)<sup>8</sup> and  $[\text{Rh}_2(\text{Cp})_2(\mu\text{-CO})(\mu\text{-C}_2(\text{CF}_3)_2)]$  (1.363 (8) Å).<sup>4c</sup> The Rh-P bond trans to the chloride ligand is significantly shorter than the other two Rh-P bonds (2.238 (5) vs 2.373 (5) Å average). The P-Rh-P angles (average 88.9 (2) Å) are slightly

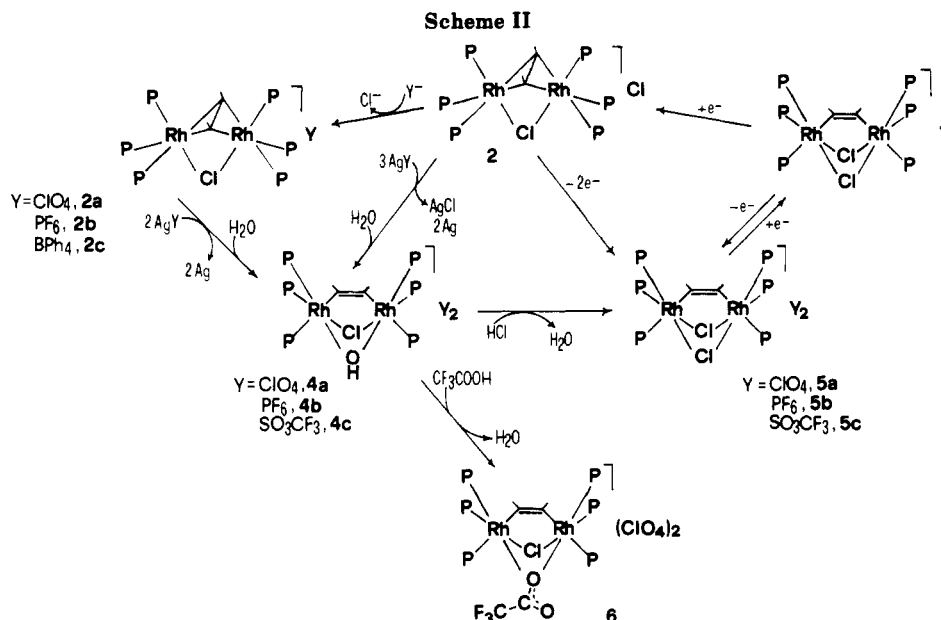
(5) Hoffman, D. M.; Hoffmann, R.; Fisel, C. R. *J. Am. Chem. Soc.* **1982**, *104*, 3858.

(6) Pauling, L. *The Nature of the Chemical Bond*, 3rd ed.; Cornell University Press: Ithaca, NY, 1960; p 230.

(7) Kutchitsu, K. *J. Chem. Phys.* **1966**, *44*, 906.

(8) Chisholm, M. H.; Foltling, K.; Huffman, J. C.; Rothwell, I. P. *J. Am. Chem. Soc.* **1982**, *104*, 4389.

(4) (a) Dickson, R. S.; Johnson, S. H.; Kirsch, H. P.; Lloyd, D. J. *Acta Crystallogr.* **1977**, *B33*, 2057. (b) Dickson, R. S.; Pain, G. N. *J. Chem. Soc., Chem. Commun.* **1979**, 277. (c) Dickson, R. S.; Pain, G. N.; Mackay, M. F. *Acta Crystallogr.* **1979**, *B35*, 2321. (d) Mague, J. T. *Organometallics* **1986**, *5*, 918. (e) Berry, D. H.; Eisenberg, R. *Organometallics* **1987**, *6*, 1796. (f) Vaartstra, B. A.; Cowie, M. *Organometallics* **1989**, *8*, 2388. (g) Breimair, J.; Steimann, M.; Wagner, B.; Beck, W. *Chem. Ber.* **1990**, *123*, 7. (h) Balch, A. L.; Fossett, L. A.; Linehan, J.; Olmstead, M. M. *Organometallics* **1986**, *5*, 691. (i) Sutherland, B. R.; Cowie, M. *Organometallics* **1984**, *3*, 1869. (j) Cowie, M.; Southern, T. G. *Inorg. Chem.* **1982**, *21*, 246. (k) Muettterties, E. L.; Pretzer, W. R.; Thomas, M. G.; Beier, B. F.; Thorn, D. L.; Day, V. W.; Anderson, A. B. *J. Am. Chem. Soc.* **1978**, *100*, 2090. (l) Muettterties, E. L.; Rhodin, T. N.; Band, E.; Brucker, C. F.; Pretzer, W. R. *Chem. Rev.* **1979**, *79*, 91.



less than  $90^\circ$ , as usually observed for the rigid (triphos)Rh fragment.<sup>3,9</sup> These structural features are quite similar to those found in the crystal structure of the mononuclear complex **1**.<sup>3</sup>

Complex **2** and all of the other congeners obtainable by substituting the chloride counteranion with  $\text{ClO}_4^-$ ,  $\text{PF}_6^-$ , or  $\text{BPh}_4^-$  (**2a-c**) are highly fluxional on the NMR time scale in solution. The variable-temperature  $^{31}\text{P}\{^1\text{H}\}$  NMR spectra in  $\text{CD}_3\text{NO}_2$  or  $\text{CD}_2\text{Cl}_2$  are reported in Figure 2. At  $95^\circ\text{C}$  the spectrum in  $\text{CD}_3\text{NO}_2$  consists of a unique broad signal centered at ca. 12 ppm. This suggests a fluxional process involving equivalence of the six phosphorus atoms of the dimer.<sup>9</sup> At lower temperature in  $\text{CD}_2\text{Cl}_2$  solution, this signal splits into two broad resonances that, at room temperature, are centered at ca. 40 (1 P) and  $-3$  ppm (2 P), respectively, with no resolvable Rh/P or P/P coupling. At the temperature range of  $-10$  to  $-40^\circ\text{C}$ , the spectrum exhibits a well-resolved  $\text{A}_2\text{MX}$  spin system with chemical shifts and coupling constants ( $\text{CD}_2\text{Cl}_2$ ,  $-25^\circ\text{C}$ ,  $\delta(\text{P}_A) -3.10$ ,  $\delta(\text{P}_M) 40.27$ ,  $J(\text{P}_A\text{P}_M) = 28.3$  Hz,  $J(\text{P}_A\text{Rh}) = 103.3$  Hz,  $J(\text{P}_M\text{Rh}) = 138.2$  Hz) that are quite comparable with those of the parent chloride  $\eta^2$ -ethylene complex **1**.<sup>3</sup> When the temperature is decreased, the resonance due to the phosphorus trans to the  $\text{C}_2\text{H}_2$  ligand ( $\text{P}_A$ ) broadens but remains practically unshifted. At  $-65^\circ\text{C}$ , the  $\text{P}_A$  resonance is completely unresolved. At lower temperature the  $\text{P}_M$  resonance also broadens, until at  $-80^\circ\text{C}$  it appears almost unresolved while the  $\text{P}_A$  resonance coalesces. Below  $-80^\circ\text{C}$ , two new signals centered at 8.5 and  $-14.5$  ppm emerge from the coalescence of  $\text{P}_A$  but do not resolved into fine structure even at  $-100^\circ\text{C}$ . However, there is little doubt that the limiting pattern is going to be AMQX.

Valuable information on the fluxionality of the dimeric cation  $[(\text{triphos})\text{Rh}(\mu\text{-Cl})(\mu\text{-}\eta^2\text{-}\eta^2\text{-C}_2\text{H}_2)\text{Rh}(\text{triphos})]^+$  (**2\***) is provided by  $^1\text{H}$  and  $^{13}\text{C}$  NMR spectra in  $\text{CD}_2\text{Cl}_2$ . At the temperature range of  $+30$  to  $-10^\circ\text{C}$ , the proton NMR spectrum shows a unique resonance centered at 2.3 ppm for the 12  $\text{CH}_2$  protons of the two triphos ligands. Below  $-10^\circ\text{C}$ , the alkyl chains of the two ligands become inequivalent, giving rise to a series of sharp resonances between 2.5 and 2.0 ppm. At the lowest temperature attained

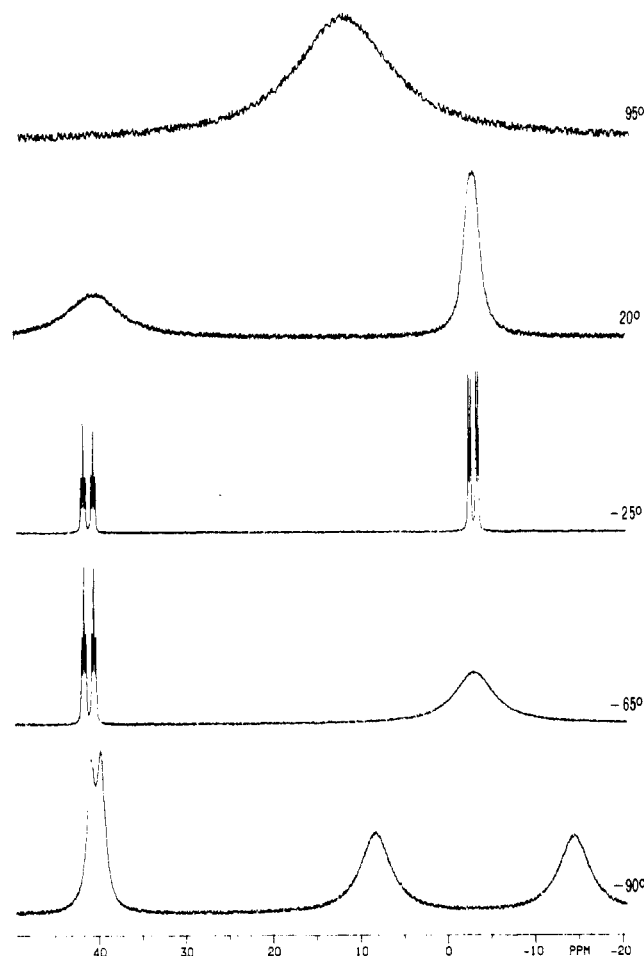


**Figure 2.** Variable-temperature  $^{31}\text{P}\{^1\text{H}\}$  NMR spectra of  $[(\text{triphos})\text{Rh}(\mu\text{-Cl})(\mu\text{-}\eta^2\text{-}\eta^2\text{-C}_2\text{H}_2)\text{Rh}(\text{triphos})]\text{Cl}$  (**2**) in  $\text{CD}_2\text{Cl}_2$ . The spectrum at  $95^\circ\text{C}$  has been recorded in  $\text{CD}_3\text{NO}_2$  (121.42 MHz, 85%  $\text{H}_3\text{PO}_4$  reference).

( $-100^\circ\text{C}$ ), the NMR pattern of the alkyl chains, although poorly resolved, appears substantially changed as expected from the  $^{31}\text{P}$  NMR results. Of particular interest is the temperature dependence of the resonance due to the ethylene hydrogens. At the temperature range of  $+30$  to  $-100^\circ\text{C}$ , these appear magnetically equivalent with a surprisingly high field chemical shift when compared with those

(9) (a) Bianchini, C.; Laschi, F.; Masi, D.; Mealli, C.; Meli, A.; Ottaviani, F. M.; Proserpio, D. M.; Sabat, M.; Zanello, P. *Inorg. Chem.* **1989**, *28*, 2552. (b) Bianchini, C.; Mealli, C.; Meli, A.; Sabat, M.; Zanello, P. *J. Am. Chem. Soc.* **1987**, *109*, 185.

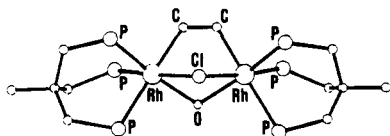


**Figure 3.** PLUTO drawing of the complex cation  $[(\text{triphos})\text{Rh}(\mu\text{-Cl})(\mu\text{-OH})(\mu\text{-}\eta^1,\eta^1\text{-C}_2\text{H}_2)\text{Rh}(\text{triphos})]^{2+}$  ( $4^{2+}$ ). All of the hydrogen atoms and phenyl rings of triphos are omitted for clarity.

of other  $\mu,\eta^2$ -ethyne complexes.<sup>1h,k,8</sup> At room temperature, the ethyne protons appear as a binomial septet at 3.30 ppm with  $J(\text{HP}) = 7.8$  Hz, thus indicating the equivalence of the six phosphorus atoms of the two triphos ligands. When the temperature is decreased, this resonance remains practically unshifted (3.13 ppm at  $-40$  °C) but changes its multiplicity, appearing as a broad quintet with a larger value of  ${}^3J(\text{HP})$  (10.8 Hz). At  $-100$  °C, the two protons are still equivalent (3.00 ppm) and appear as an unresolved multiplet.

Finally, and in line with the proton spectra, a single ethyne carbon resonance at 50.0 ppm ( $J(\text{CH}) = 199.0$  Hz) is found in the gate-off decoupled  ${}^{13}\text{C}$  NMR spectrum at room temperature, which suggests a carbon hybridization lying between  $\text{sp}^2$  and  $\text{sp}^3$ .<sup>1h,k,8</sup>

Inspection of the structural and NMR data indicates that  $2^+$  in solution maintains the  $C_{2v}$  symmetry and undergoes two different fluxional processes with different activation energies, which first interconvert two  ${}^{31}\text{P}$  sites (lower  $E_a$ ) and then three  ${}^{31}\text{P}$  sites (higher  $E_a$ ).

**Reactions of  $[(\text{triphos})\text{Rh}(\mu\text{-Cl})(\mu\text{-}\eta^2,\eta^2\text{-C}_2\text{H}_2)\text{Rh}(\text{triphos})]\text{Cl}$  with Oxidants.** As anticipated in the preceding section, **2** readily undergoes metathetical reactions with a variety of salts such as  $(\text{NBu}_4)\text{ClO}_4$ ,  $\text{TlPF}_6$ , and  $\text{NaBPh}_4$  to give  $[(\text{triphos})\text{Rh}(\mu\text{-Cl})(\mu\text{-}\eta^2,\eta^2\text{-C}_2\text{H}_2)\text{Rh}(\text{triphos})]\text{Y}$  ( $\text{Y} = \text{ClO}_4$  (**2a**),  $\text{PF}_6$  (**2b**),  $\text{BPh}_4$  (**2c**)). When the substitution of the  $\text{Cl}^-$  counteranion is attempted with a 3-fold excess of a silver(I) salt such as  $\text{AgClO}_4$ ,  $\text{AgPF}_6$ , or  $\text{AgSO}_3\text{CF}_3$ , the elimination of  $\text{Cl}^-$  is accompanied by two-electron oxidation of the complex (Scheme II). In the absence of external ligands, the oxidation product is not stable per se and rapidly decomposes unless a wet solvent is used. In this case, the product extracts a hydroxy ligand from water, thereby saturating its coordination sphere. As a result, orange crystalline compounds of general formula  $[(\text{triphos})\text{Rh}(\mu\text{-Cl})(\mu\text{-OH})(\mu\text{-}\eta^1,\eta^1\text{-C}_2\text{H}_2)\text{Rh}(\text{triphos})](\text{Y})_2$  ( $\text{Y} = \text{ClO}_4$  (**4a**),  $\text{PF}_6$  (**4b**),  $\text{SO}_3\text{CF}_3$  (**4c**)) are obtained in good yields. When less than 3 equiv of silver(I) salt is used, variable mixtures of **4a-c** and of the  $(\mu\text{-Cl})_2$  isomers  $[(\text{triphos})\text{Rh}(\mu\text{-Cl})_2(\mu\text{-}\eta^1,\eta^1\text{-C}_2\text{H}_2)\text{Rh}(\text{triphos})](\text{Y})_2$  ( $\text{Y} = \text{ClO}_4$  (**5a**),  $\text{PF}_6$  (**5b**),  $\text{SO}_3\text{CF}_3$  (**5c**)) are obtained (see below). Alternatively, complexes **4a,b** can be prepared by reacting **2a,b** with a 2-fold excess of the appropriate silver(I) salt in reagent grade acetone.

Complexes **4a-c** are fairly stable in both the solid state and solution, where they behave as 1:2 electrolytes. Crystals suitable for an X-ray analysis were obtained by recrystallization of **4c** from a 1:1:2 mixture of acetone, benzene, and 1-butanol. Unfortunately, an acceptable refinement of the structure was precluded because of high disorder affecting the triflate counteranions. Actually, the refinement converged to  $R = 0.10$ .<sup>10</sup> Although the

(10) Crystal data: monoclinic,  $P2_1/n$  (No. 14),  $a = 24.700$  (5) Å,  $b = 24.800$  (6) Å,  $c = 16.854$  (5) Å,  $\beta = 91.01$  (6)°,  $V = 10335.8$  Å<sup>3</sup>,  $Z = 4$ . Data were collected on a Philips PW 1100 diffractometer with  $\text{Mo K}\alpha$  radiation. Of the 10378 total measured reflections, 2831 having  $I \geq 3\sigma(I)$  were considered observed. The structure was solved by Patterson and Fourier techniques and refined to  $R = 0.10$ . Anisotropic temperature factors for Rh and P atoms were used in the least-squares refinement. Phenyl rings were treated as rigid bodies of  $D_{6h}$  symmetry.

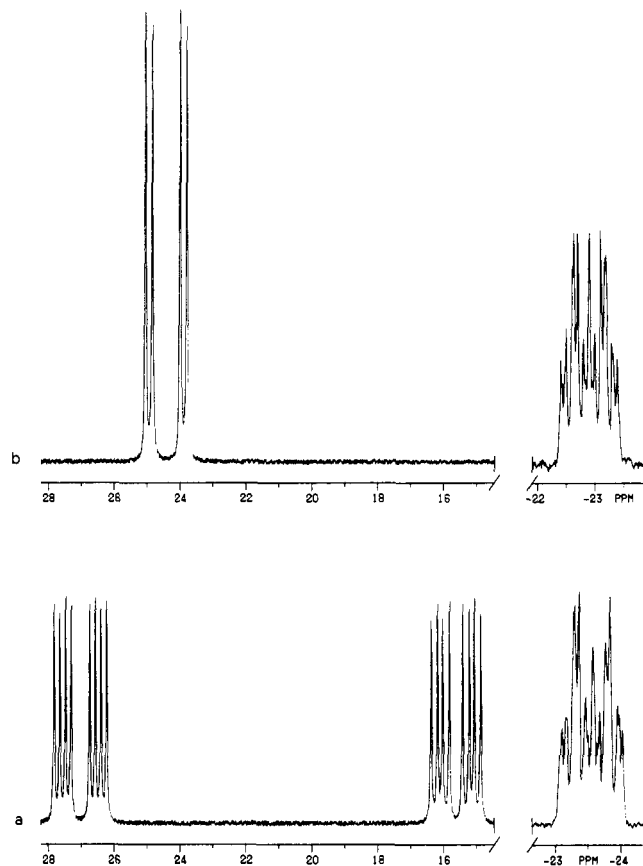


**Figure 4.**  ${}^{31}\text{P}\{^1\text{H}\}$  NMR spectra of (a)  $[(\text{triphos})\text{Rh}(\mu\text{-Cl})(\mu\text{-OH})(\mu\text{-}\eta^1,\eta^1\text{-C}_2\text{H}_2)\text{Rh}(\text{triphos})](\text{PF}_6)_2$  (**4b**) and (b)  $[(\text{triphos})\text{Rh}(\mu\text{-Cl})_2(\mu\text{-}\eta^1,\eta^1\text{-C}_2\text{H}_2)\text{Rh}(\text{triphos})](\text{PF}_6)_2$  (**5b**) (121.42 MHz, 20 °C,  $\text{CD}_2\text{Cl}_2$ , 85%  $\text{H}_3\text{PO}_4$  reference).

structural data for **4c** cannot be published in the present form, there is little doubt about the reliability of the structure shown in the PLUTO drawing presented in Figure 3. In the structure, each rhodium has a slightly distorted octahedral geometry in which the coordination sites are occupied by triphos, a bridging chloride, a bridging hydroxy ligand, and one end of the bridging acetylene group, bound as a cis-dimetalated olefin. The Rh-Rh separation of 3.378 (5) Å still corresponds to no formal metal-metal bond. The structure is thus analogous to a number of  $\mu\text{-}\eta^1,\eta^1$ -acetylene complexes exhibiting the same face-sharing bioctahedral geometry, namely  $[\text{Fe}_2(\text{CO})_6(\mu\text{-SCF}_3)(\mu\text{-C}_2(\text{CF}_3)_2)]^{11a}$  and  $[\text{Ir}(\text{CO})(\text{PMe}_3)(\mu\text{-S-}t\text{-Bu})(\mu\text{-C}_2\text{R}_2)]$  ( $\text{R} = \text{CF}_3$ ,  $\text{CH}_3\text{OC}(\text{O})$ ).<sup>11b</sup>

Since the counteranion does not at all influence the NMR spectroscopic properties of **4a-c**, these are considered, from now on, as a unique entity. In solution the complex cation  $[(\text{triphos})\text{Rh}(\mu\text{-Cl})(\mu\text{-OH})(\mu\text{-}\eta^1,\eta^1\text{-C}_2\text{H}_2)\text{Rh}(\text{triphos})]^{2+}$  ( $4^{2+}$ ) exhibits spectroscopic properties consistent with the structure shown in Figure 3. The  ${}^{31}\text{P}\{^1\text{H}\}$  NMR spectrum in  $\text{CD}_2\text{Cl}_2$  is temperature-invariant from  $+35$  to  $-90$  °C and shows an  $[\text{AMQX}]_2$  spin system, indicating that the three phosphorus atoms around each rhodium are inequivalent (Figure 4a). Interestingly, the two phosphorus nuclei trans to the carbons of the metalated olefin ( $\text{P}_Q$ ) are strongly coupled to each other and to the rhodium nuclei as well. In fact, the  $\text{P}_Q$  resonance can be properly computed as the  $\text{QQ}'$  part of an  $\text{AA}'\text{MM}'\text{QQ}'\text{XX}'$  system with  $J(\text{P}_Q\text{P}_{Q'}) = 10.7$  Hz and

(11) (a) Davidson, J. L.; Harrison, W.; Sharp, D. W. A.; Sim, G. A. *J. Organomet. Chem.* **1972**, *46*, C47. (b) Amanc, M. E.; Mathieu, R.; Poilblanc, R. *Organometallics* **1983**, *2*, 1618.

Table II.  $^{31}\text{P}\{^1\text{H}\}$  NMR Data<sup>a</sup>

compd	pattern	chem shift, $\delta(\text{P})$ , ppm	coupling const., Hz <sup>b</sup>				
			PRh		PP		
2	$\text{A}_2\text{X}^c$	$\text{P}_A$	12.00				
		$\text{P}_A$	-3.10	$\text{P}_A\text{Rh}$	103.3	$\text{P}_A\text{P}_M$	28.3
	AMQX <sup>e</sup>	$\text{P}_M$	40.27	$\text{P}_M\text{Rh}$	138.2		
		$\text{P}_A$	-14.5				
		$\text{P}_M$	8.5				
4b	$[\text{AMQX}]_2$	$\text{P}_Q$	40.1				
		$\text{P}_A$	27.02	$\text{P}_A\text{Rh}$	131.1	$\text{P}_A\text{P}_M$	42.3
		$\text{P}_M$	15.63	$\text{P}_M\text{Rh}$	115.7	$\text{P}_A\text{P}_Q$	21.6
		$\text{P}_Q$	-23.39	$\text{P}_Q\text{Rh}$	58.8	$\text{P}_M\text{P}_Q$	23.2
5b	$[\text{A}_2\text{MX}]_2$	$\text{P}_Q$	3.2	$\text{P}_Q\text{Rh}$	10.7		
		$\text{P}_A$	23.47	$\text{P}_A\text{Rh}$	127.2	$\text{P}_A\text{P}_M$	24.6
		$\text{P}_M$	-22.90	$\text{P}_M\text{Rh}$	60.8	$\text{P}_A\text{P}_M'$	0.4
				$\text{P}_M\text{Rh}$	3.2	$\text{P}_M\text{P}_M'$	11.7
6	$[\text{AMQX}]_2$	$\text{P}_A$	25.55	$\text{P}_A\text{Rh}$	132.2	$\text{P}_A\text{P}_M$	39.4
		$\text{P}_M$	22.60	$\text{P}_M\text{Rh}$	127.6	$\text{P}_A\text{P}_Q$	19.2
		$\text{P}_Q$	-23.62	$\text{P}_Q\text{Rh}$	60.2	$\text{P}_M\text{P}_Q$	26.5
				$\text{P}_Q\text{Rh}$	2.8	$\text{P}_Q\text{P}_Q$	10.4

<sup>a</sup>In  $\text{CD}_2\text{Cl}_2$  at 20 °C. <sup>b</sup>The spectra of **4b**, **5b**, and **6** have been computed by considering an additional coupling constant of ca. 0.1 Hz between the two magnetically inequivalent rhodium atoms. <sup>c</sup>In  $\text{CD}_3\text{NO}_2$  at 95 °C. <sup>d</sup>-25 °C. <sup>e</sup>-90 °C.

$J(\text{P}_Q\text{Rh}) = 3.2$  Hz (for the other NMR data see Table II). In the  $^1\text{H}$  NMR spectrum recorded in  $\text{CD}_2\text{Cl}_2$ , the ethyne hydrogens appear as a multiplet at 6.83 ppm with no discernable coupling because of partial superimposition of the signal with the resonances of the phenyl hydrogens. A well-resolved, high-field septet at -0.54 ppm can be reasonably assigned to the OH hydrogen,<sup>12</sup> which exhibits an equivalent long-range coupling to the six phosphorus nuclei of the complex ( $^3J(\text{HP}) = 1.8$  Hz). The  $^{13}\text{C}\{^1\text{H}\}$  NMR spectrum in  $\text{CD}_3\text{NO}_2$  at room temperature shows the two ethyne carbons to be equivalent. These appear as a doublet of doublets of multiplets at surprisingly low field ( $\delta$  165.1 ppm;  $^1J(\text{CRh}) = 93.4$  Hz,  $^2J(\text{CP}) = 17.6$  Hz). A gated decoupling experiment gave a  $J(\text{CH})$  value of 162.8 Hz. A reliable comparison of the present  $^{13}\text{C}$  NMR parameters with those reported for other metal-( $\mu$ - $\eta^1$ , $\eta^1$ - $\text{C}_2\text{R}_2$ ) complexes is precluded by the scarcity of literature data, especially for rhodium compounds.<sup>13</sup>

In addition to NMR and IR evidence ( $\nu(\text{OH})$  3665, 3580  $\text{cm}^{-1}$ ),<sup>12</sup> the presence of a bridging hydroxy ligand in **4a** is shown by the reaction in  $\text{CH}_2\text{Cl}_2$  with  $\text{CF}_3\text{COOH}$ , which gives  $\text{H}_2\text{O}$  and the  $\mu$ -carboxylate complex [(triphos)Rh( $\mu$ - $\text{O}_2\text{CCF}_3$ )( $\mu$ -Cl)( $\mu$ - $\eta^1$ , $\eta^1$ - $\text{C}_2\text{H}_2$ )Rh(triphos)]( $\text{ClO}_4$ )<sub>2</sub> (**6**). Monitoring the reaction between **4a** and  $\text{CF}_3\text{COOH}$  in  $\text{CD}_2\text{Cl}_2$  in an NMR tube shows formation of HDO. The spectroscopic properties of **6** are quite comparable with those exhibited by **4a-c** (see Table II and Experimental Section). The resonance of the ethyne hydrogens is now discernable at 6.33 ppm with  $J(\text{HRh}) = 7.9$  Hz and  $J(\text{HP}) = 11.3$  Hz. The IR spectrum contains  $\nu(\text{C}=\text{O})$  at 1654  $\text{cm}^{-1}$ , indicating a carboxylate group bridging through one oxygen atom.<sup>14</sup>

Displacement of the  $\mu$ -hydroxy group by other ligands with retention of the primary geometry of the complex can also be achieved by reacting **4a-c** with gaseous HCl. In this case, the double-chloride-bridged complexes **5a-c** form in quantitative yield. Alternatively, complex **5b** can be straightforwardly prepared by treatment of the  $\mu$ - $\eta^2$ , $\eta^2$ -

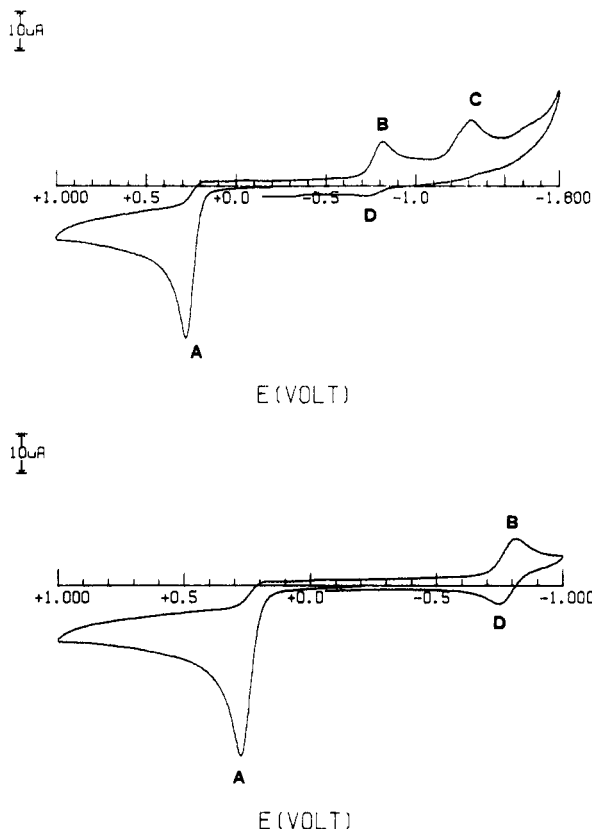


Figure 5. Cyclic voltammograms recorded at a platinum electrode on a deaerated  $\text{CH}_2\text{Cl}_2$  solution containing **2** ( $1.45 \times 10^{-3}$  mol  $\text{dm}^{-3}$ ) and  $[\text{NBu}_4]\text{ClO}_4$  (0.2 mol  $\text{dm}^{-3}$ ). The scan rate was 0.2  $\text{V s}^{-1}$ .

$\text{C}_2\text{H}_2$  complex **2** in  $\text{CH}_2\text{Cl}_2$  with 2 equiv of  $[(\text{Cp})_2\text{Fe}]\text{PF}_6$ . The structural formulation of **5a-c** as given in Scheme II is strongly supported by  $^{31}\text{P}$ ,  $^{13}\text{C}$ , and  $^1\text{H}$  NMR spectra. The  $^{31}\text{P}\{^1\text{H}\}$  NMR spectrum in  $\text{CD}_2\text{Cl}_2$  is shown in Figure 4b. The  $[\text{A}_2\text{MX}]_2$  spin system is temperature-invariant from +35 to -90 °C and consistent with a structure where two phosphorus nuclei of each triphos are mutually equivalent, as is the case of the phosphorus trans to the two Cl bridges. Like the spectra of **4a-c** and **6**, the two phosphorus atoms trans to the bridging  $\text{C}_2\text{H}_2$  moiety are coupled to each other and to the two rhodium nuclei. Indeed, the resonance of  $\text{P}_M$  can be computed as the MM' part of an  $\text{A}_2\text{A}_2'\text{MM}'\text{XX}'$  spin system. The occurrence of a significant long-range coupling between phosphorus or rhodium nuclei belonging to different (triphos)Rh fragments is not of trivial importance, as one should recall that such couplings have not been found for the  $\mu$ - $\eta^2$ , $\eta^2$ - $\text{C}_2\text{H}_2$  precursors. Accordingly, it is possible that such long-range couplings may be taken as a diagnostic tool to distinguish the  $\mu$ - $\eta^1$ , $\eta^1$ - $\text{C}_2\text{H}_2$  bonding mode from the  $\mu$ - $\eta^2$ , $\eta^2$ - $\text{C}_2\text{H}_2$  mode in  $\mu$ -acetylene complexes containing P and/or Rh.

The ethyne hydrogens and carbons in **5a-c** are magnetically equivalent in the +35 to -90 °C range, as shown by  $^1\text{H}$  and  $^{13}\text{C}\{^1\text{H}\}$  NMR spectra in  $\text{CD}_2\text{Cl}_2$ , which are quite comparable with those of **4a-c** and **6** (see Experimental Section). In particular, the resonance of the ethyne hydrogens appears as a well-resolved multiplet (dq) at 6.61 ppm with  $J(\text{HP}_M) = 28.4$  and  $J(\text{HP}_A) = J(\text{HRh}) = 14.9$  Hz.

**Electrochemical Studies.** Having discovered that two-electron oxidation of **2** affects both the structure and chemistry of the complex, we decided to study the redox behavior of the present family of  $\mu$ - $\eta^2$ , $\eta^2$ - $\text{C}_2\text{H}_2$  and  $\mu$ - $\eta^1$ , $\eta^1$ - $\text{C}_2\text{H}_2$  (ethyne)dirhodium complexes, by electrochemical methods.

(12) Cabeza, J. A.; Smith, A. J.; Adams, H.; Maitlis, P. M. *J. Chem. Soc., Dalton Trans.* 1986, 1155.

(13) Burn, M. J.; Kiel, G. Y.; Seils, F.; Takats, J.; Washington, J. J. *Am. Chem. Soc.* 1989, 111, 6850.

(14) Bianchini, C.; Meli, A.; Peruzzini, M.; Zanobini, F.; Zanello, P. *Organometallics* 1990, 9, 241.

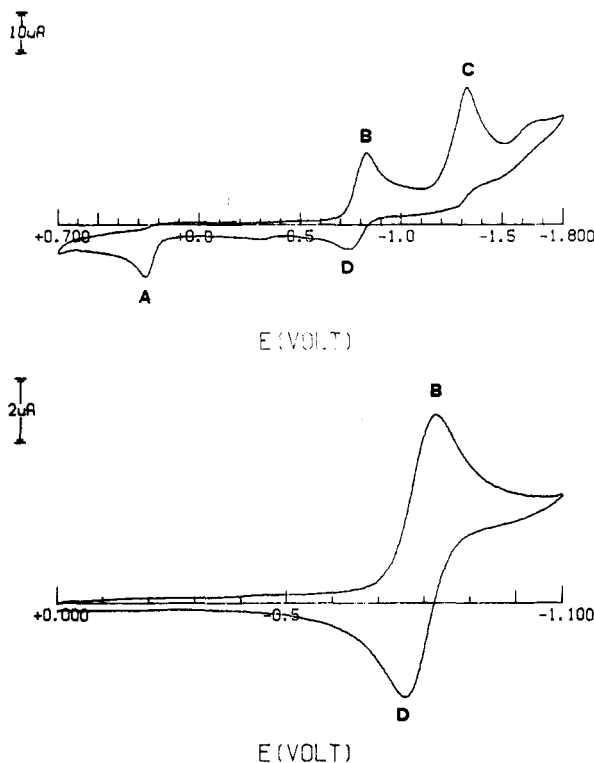


**Figure 6.** Cyclic voltammograms recorded at a platinum electrode on a deaerated  $\text{CH}_2\text{Cl}_2$  solution containing **5a** ( $1.25 \times 10^{-3}$  mol  $\text{dm}^{-3}$ ) and  $[\text{NBu}_4]\text{ClO}_4$  ( $0.2$  mol  $\text{dm}^{-3}$ ): (a) scan rate  $0.2$   $\text{V s}^{-1}$ ; (b) scan rate  $0.02$   $\text{V s}^{-1}$ .

As shown in Figure 5, which illustrates the redox pattern of **2** in  $\text{CH}_2\text{Cl}_2$ , the complex undergoes an oxidation process in correspondence to peak A ( $E_p = +0.28$  V). This does not display a directly associated reduction response in the reverse scan but two consecutive reduction steps at peaks B and C, respectively, very far from it. In turn, peak B exhibits a directly associated response, peak D, in the reverse scan.

Controlled-potential coulometric tests at  $E_w = +0.6$  V indicate that the oxidation process consumes 2 faraday/mol. After exhaustive two-electron removal, the resulting yellow solution displays a cyclic voltammogram fully coincident with that obtained with an authentic sample of  $[(\text{triphos})\text{Rh}(\mu\text{-Cl})_2(\mu\text{-}\eta^1, \eta^1\text{-C}_2\text{H}_2)\text{Rh}(\text{triphos})](\text{ClO}_4)_2$  (**5a**) (Figure 6). The electrogenerated cation  $5^{2+}$  undergoes two subsequent reduction processes. The first one exhibits a directly associated reoxidation, in the reverse scan, indicating a chemically reversible redox change. The second one restores **2** (see the appearance of peak A).

In spite of the apparent chemical reversibility of the  $5^{2+}/5^+$  redox change occurring at the peak system B/D, controlled-potential coulometry ( $E_w = -0.95$  V) shows that, after the consumption of one electron/molecule, the electrolysis current abruptly drops but remains slightly higher than the background current up to the overall spending of two electrons/molecule. Cyclic voltammetric tests performed after the consumption of either one or two electrons/molecule provide evidence for the presence of the oxidation peak A. This means that  $2^+$  is regenerated not only by reduction of  $5^{2+}$  at the second cathodic step (see Figure 6) but also by  $5^+$  through a slow chemical reaction. In order to prevent this slow chemical complication, controlled-potential electrolysis was performed at low temperature ( $-20$  °C). Indeed, the electrolysis current substantially stops after the consumption of one electron/molecule at  $E_w = -0.9$  V and, on the basis of its peak height,  $2^+$  is now regenerated only in a 10% yield with

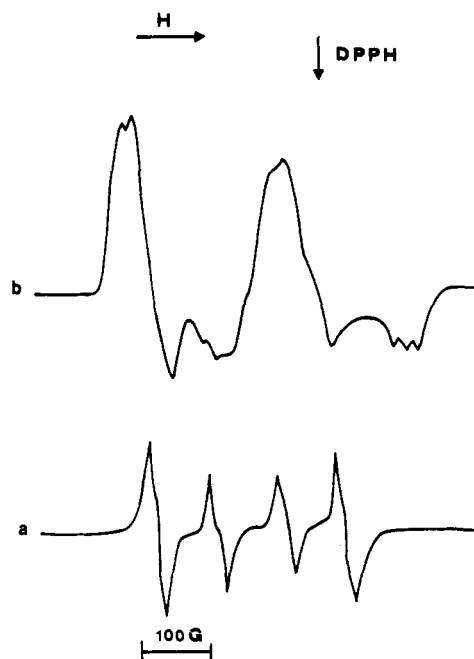


**Figure 7.** X-Band ESR spectra of electrogenerated  $5^+$  in  $\text{CH}_2\text{Cl}_2$  at (a)  $-100$  °C and (b)  $-20$  °C.

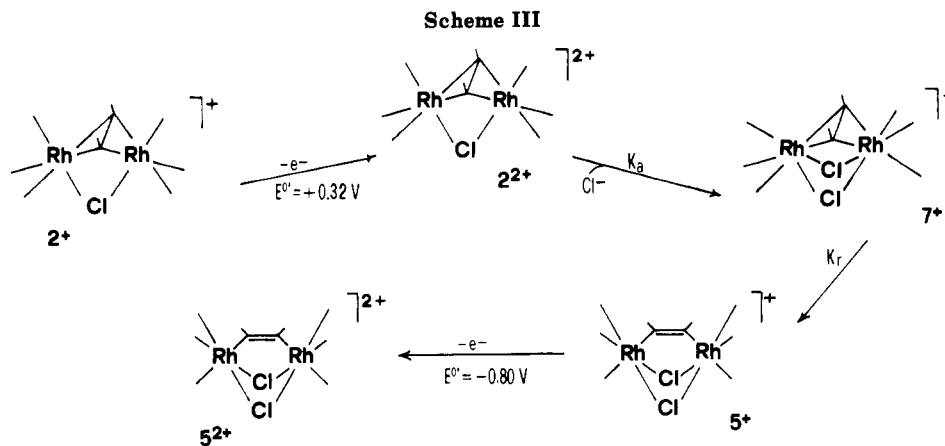
respect to the final amount regenerated by further one-electron reduction at the potential of the second cathodic process ( $E_w = -1.5$  V). A slow disproportionation reaction of  $5^+$  to generate  $2^+$  and  $5^{2+}$  might well explain this behavior.

Valuable information on the electronic structure of the product obtained by one-electron reduction of  $5^{2+}$  is provided by ESR spectroscopy. The frozen X-band ESR spectrum in  $\text{CH}_2\text{Cl}_2$  at  $-100$  °C of electrogenerated  $5^+$  is shown in Figure 7a. The spectrum can be interpreted by using a  $S = 1/2$  spin Hamiltonian with  $g_{\parallel} = 2.010$  ( $A_{\parallel} = 286$  G) and  $g_{\perp} = 2.082$  ( $A_{\perp} = 226$  G). A three-line resolution is present in each perpendicular ( $A_{\perp} = 30$  G) and parallel ( $A_{\parallel} = 15$  G) absorption. As has been recently reported for the mononuclear complexes  $[(\text{triphos})\text{Rh}(\text{S}_2\text{CO})]^{15}$  and  $[(\text{triphos})\text{Rh}(\text{CH}(\text{CO}_2\text{Me})\text{CH}_2(\text{CO}_2\text{Me}))]^{16}$ , the present set of ESR parameters is strongly diagnostic for a low-spin Rh(II) structure with the unpaired electron in the  $d_{z^2}$  orbital. In particular, the largest  $A_{\parallel}$  and  $A_{\perp}$  values have been assigned to a strong interaction of the electron with the phosphorus looking at the  $d_{z^2}$  SOMO.<sup>15,16</sup> This may occur also in complexes having an octahedral structure about Rh(II), as is the case for  $5^+$ . In this case, the splitting observed in the perpendicular and parallel absorptions can be attributed to interaction of the electron with the two equivalent basal phosphorus atoms. In fluid solution,  $5^+$  is fluxional on the ESR time scale. At  $-20$  °C, the spectrum consists of four lines centered at  $(g)$  2.069 ( $\langle A_{\perp} \rangle = 95$  G) with an intensity ratio of 2:1:1:2 (Figure 7b). When the temperature is increased, the intensity ratio becomes closer to 1:3:3:1, as one would expect for coupling of the unpaired electron to three equivalent phosphorus nuclei.<sup>15-17</sup> Unfortunately, the spectrum at room temperature could not be recorded due to fast decomposition of the complex.

(15) Bianchini, C.; Meli, A.; Laschi, F.; Vizza, F.; Zanello, P. *Inorg. Chem.* 1989, 28, 227.

(16) Bianchini, C.; Laschi, F.; Meli, A.; Peruzzini, M.; Zanello, P.; Frediani, P. *Organometallics* 1988, 7, 2575.

(17) Casagrande, L. V.; Chen, T.; Rieger, P. H.; Robinson, B. H.; Simpson, J.; Visco, S. J. *Inorg. Chem.* 1984, 23, 2019. DeGray, J. A.; Meng, Q.; Rieger, P. H. *J. Chem. Soc., Faraday Trans. 1* 1987, 83, 3565.



To summarize, the ESR data indicate that the unpaired electron is localized on a rhodium(II) center. Accordingly, if we assume a formal Rh(II)–Rh(III) configuration for  $5^+$ , the parent complex  $5^{2+}$  must be formulated as containing a Rh(III)–Rh(III) core, which is in agreement with previous reports.<sup>5</sup> At this point, one may dispute the formal oxidation state of the two rhodium atoms along the illustrated redox pathway. The problem is not really important, as much depends on the formalism used to count the electrons on the metals and ethyne as well. Given that  $5^{2+}$  is  $d^6$ – $d^6$ , i.e. Rh(III)–Rh(III), then the one-electron-reduced species is Rh(II)–Rh(III), which is consistent with the ESR data. Also, this interpretation would reasonably imply a Rh(III)–Rh(III) core for the starting  $2^+$  complex and, therefore, would suggest an ethyne-centered two-electron oxidation (a Rh(IV)–Rh(IV) structure is most unlikely if one considers the nature of the ligands). Alternatively, one may think of  $2^+$  as containing a Rh(I)–Rh(I) core that transforms into Rh(II)–Rh(II) by two-electron oxidation. We are inclined to prefer the former hypothesis, especially after analyzing the  $^{31}\text{P}$  NMR parameters of **2**, which are almost coincident with those of **1**, where a Rh(III) metallocyclopropane structure was established on the basis of a single-crystal X-ray analysis.<sup>3</sup>

Also, it is worth mentioning that the  $2^+/5^{2+}$  interconversion much resembles that previously reported for the ethenetetrathiolate ( $\text{C}_2\text{S}_4^{4-}$ ) complex  $[(\text{triphos})\text{Rh}(\mu\text{-C}_2\text{S}_4)\text{Rh}(\text{triphos})]^{2+}$  and the tetrathiooxalate ( $\text{C}_2\text{S}_4^{2-}$ ) complex  $[(\text{triphos})\text{Rh}(\mu\text{-C}_2\text{S}_4)\text{Rh}(\text{triphos})]^{4+}$ .<sup>9b</sup>

Now we must face up to the problem of the mechanistic aspects of the chemically reversible pathway connected to the interconversion  $2^+/5^{2+}$  through clearly significant stereodynamics. It is evident that the single-stepped two-electron removal from  $2^+$  must be accompanied by both chemical association of the chloride counteranion ( $C_a$ ) and geometrical reorganization ( $C_r$ ) to  $5^{2+}$ . In principle, this step can occur alternatively by an EECC, ECCE, or ECEC mechanism, where E represents an electron transfer and C represents the observed chemical or stereochemical process. Indeed, we have some evidence for an  $\text{EC}_a\text{C}_r\text{E}$  mechanism of the type reported in Scheme III. In fact, cyclic voltammetric tests on **2** at scan rates ( $\nu$ ) varying from 0.02 to ca. 50  $\text{V s}^{-1}$  show that no associated response to peak A is detectable in the reverse scan up to 20  $\text{V s}^{-1}$ , whereas at 20.48  $\text{V s}^{-1}$ , a directly associated reduction peak appears with an  $i_{pc}/i_{pa}$  ratio of about 0.4, which increases further to 0.5 at 51.2  $\text{V s}^{-1}$ . This finding allows one to approximately evaluate the formal electrode potential (+0.32 V) for the couple  $2^+/2^{2+}$ . In addition, chronoamperometric tests in the range from 1 ms to 2 s show that  $n_{app}$  ( $it^{1/2}$ ) increases from 1.6 to 2.0 over the 3–21-ms range, at which point it remains constant. This means that the

very fast chemical complications following the  $2^+/2^{2+}$  oxidation take place within 20 ms after the first one-electron removal. Further mechanistic information is provided by the back-conversion of  $5^{2+}$  to  $2^+$  through two separated one-electron reductions. In this connection, analysis of the response relevant to the  $5^{2+}/5^+$  redox change with scan rate at room temperature reveals the following: (i) the current ratio  $i_{p(D)}/i_{p(B)}$  is constantly equal to 1; (ii) the peak-to-peak separation,  $\Delta E_p$ , progressively increases from 66 mV at 0.02  $\text{V s}^{-1}$  to 295 mV at 20.48  $\text{V s}^{-1}$ ; (iii) the current function  $i_{p(B)}\nu^{-1/2}$  remains substantially constant. These features are diagnostic<sup>18</sup> for a simple, essentially reversible, one-electron transfer in the cyclic voltammetric time scale and indicate that  $5^+$  maintains a molecular geometry substantially similar to that of  $5^{2+}$  (note that, under the same experimental conditions, the assumed reversible one-electron oxidation of ferrocene exhibits a quite coincident increase of  $\Delta E_p$  with scan rate).<sup>19</sup> Unfortunately, all our attempts to isolate  $5^+$  as the perchlorate salt were unsuccessful because of the disproportionation reaction occurring in the longer time window of macroelectrolysis. It is therefore evident that, at the potentials of the first one-electron removal, once  $5^+$  forms through stereochemically favored reorganizational processes, its further one-electron oxidation to  $5^{2+}$  occurs.

The compound  $[(\text{triphos})\text{Rh}(\mu\text{-Cl})(\mu\text{-}\eta^2, \eta^2\text{-C}_2\text{H}_2)\text{Rh}(\text{triphos})]\text{PF}_6$  (**2b**), which differs from **2** only in having a noncoordinating counteranion, displays a redox behavior only apparently similar to that of **2**. In fact, it undergoes an anodic process at peak A ( $E_p = +0.42$  V), which exhibits in the reverse scan an associated reduction peak B and some other minor responses at more negative potentials. Further inversion of the scan direction leads to a predominant oxidation peak E at a potential ( $E_p = +0.33$  V) significantly different from that of the initial peak A. This suggests that, unlike **2**, **2b** cannot be restored upon oxidation/reduction cycles. Once again, controlled-potential coulometry indicates that the oxidation of **2b** ( $E_w = +0.6$  V) involves an overall two-electron step. After exhaustive two-electron oxidation performed at  $-20$  °C, the resulting solution gives rise to a cyclic voltammetric picture coincident with that exhibited by an authentic sample of  $[(\text{triphos})\text{Rh}(\mu\text{-Cl})(\mu\text{-OH})(\mu\text{-}\eta^1, \eta^1\text{-C}_2\text{H}_2)\text{Rh}(\text{triphos})](\text{PF}_6)_2$  (**4b**). This shows a first, apparently chemically reversible one-electron reduction ( $E^{o'} = -1.09$  V), followed by a second irreversible one-electron addition ( $E_p = -1.46$  V). However, we failed in obtaining an ESR response for the

(18) Brown, E. R.; Sandifer, J. R. In *Physical Methods of Chemistry*; Rossiter, B. W., Hamilton, J. F., Eds.; Wiley: New York, 1986; Vol. 2, Chapter 4.

(19) Geiger, W. E. *Prog. Inorg. Chem.* 1985, 33, 275.



one-electron reduction  $4^+$  product obtained by exhaustive reduction at  $-1.2$  V.

Analysis of the peak system A/B exhibited by **2b** with scan rate shows that the  $i_{p(B)}/i_{p(A)}$  ratio progressively increases from 0.6 at  $0.02$  V  $s^{-1}$  to ca. 1 at  $5.12$  V  $s^{-1}$  while the current function  $i_{p(A)}v^{-1/2}$  progressively decreases. Concomitantly,  $\Delta E_p$  increases from 102 to 310 mV. If allowance is made to assign again the overall two-electron oxidation to an ECE mechanism, then one may infer that the chemical complications following the  $2b^+/2b^{2+}$  redox change are notably slower than those occurring after the  $2^+/2^{2+}$  charge transfer (note that the formal electrode potential is almost coincident for the two systems). This is not really unexpected, since now the electronically unsaturated complex  $2b^{2+}$  is not surrounded by additional ligands as is the case for  $2^{2+}$ , which converts into  $7^+$  by incorporation of the  $Cl^-$  counteranion. The voltammetric resemblance with **4b** confirms the chemical evidence that hydroxo groups are extracted from adventitious water in the solvent. Finally, the quasi-reversibility of the  $2b^+/2b^{2+}$  oxidation suggests that, upon one-electron removal, significant geometrical strain is intrinsically induced in the complex framework, as it likely occurs as soon as the first electron is removed from **2**.

### Conclusions

The present study, through an accumulation of a body of experimental data, sheds some light on a well-documented example of interconversion between  $\mu-\eta^2, \eta^2$  and  $\mu-\eta^1, \eta^1$  bonding modes of acetylene. The transformation is strictly controlled by the overall electron count in the dimeric framework and requires an additional ligand to stabilize the  $\mu-\eta^1, \eta^1$ -acetylene complex. The *noninnocent* character of the ethyne ligand becomes transparent: formally, it can be reasonably formulated as  $C_2H_2^{4-}$  in the  $\mu-\eta^2, \eta^2$  complex or as  $C_2H_2^{2-}$  in the  $\mu-\eta^1, \eta^1$  derivative. Finally, we have accumulated a body of experimental evidence pointing to an  $EC_aC_rE$  mechanism for the chemically reversible pathway  $M(\mu-\eta^2, \eta^2-C_2H_2) \rightleftharpoons M(\mu-\eta^1, \eta^1-C_2H_2)$ .

### Experimental Section

**General Information.** All reactions and manipulations were routinely performed under a nitrogen atmosphere by using Schlenk-line techniques. The solid compounds were collected on sintered-glass frits and washed with appropriate solvents before being dried under a stream of nitrogen. Reagent grade chemicals were used in the preparations of the complexes. THF and  $CH_2Cl_2$  were purified by distillation over  $LiAlH_4$  and  $P_2O_5$  under nitrogen just prior to use, respectively. The compounds  $[(\text{triphos})RhCl(C_2H_4)]^3$  and  $[(\text{Cp})_2Fe]PF_6^{20}$  were prepared according to published procedures.

Infrared spectra were recorded on a Perkin-Elmer 1600 Series FTIR spectrophotometer using samples milled in Nujol between KBr plates.

Proton and  $^{13}C\{^1H\}$  NMR spectra were recorded at 299.945 and 75.429 MHz, respectively, on a Varian VXR 300 spectrometer. Peak positions are relative to tetramethylsilane as external reference.  $^{31}P\{^1H\}$  NMR spectra were recorded on a Varian VXR 300 instrument operating at 121.42 MHz. Chemical shifts are relative to external 85%  $H_3PO_4$ , with downfield values reported as positive. Simulation of NMR spectra was achieved by using an updated version of the DAVINS program.<sup>21</sup> The initial choices of shifts and coupling constants were refined by iterative least-squares calculation with use of the experimental digitized spec-

trum. The final parameters gave a satisfactory fit between experimental and calculated spectra, the agreement factor  $R$  being 0.95%.

Conductivities were measured with an ORION Model 990101 conductance cell connected to a Model 101 conductivity meter. The conductivity data were obtained at sample concentrations of ca.  $10^{-3}$  M in nitroethane solutions.

Cyclic voltammetry was performed in a three-electrode cell having a platinum working electrode surrounded by a platinum-spiral counter electrode, and the aqueous saturated calomel reference electrode (SCE) mounted with a Luggin capillary. Either a BAS 100A electrochemical analyzer or a multipurpose Amel instrument (a Model 566 analog function generator and a Model 552 potentiostat) was used as the polarizing unit. Controlled-potential coulometric tests were performed in an H-shaped cell with anodic and cathodic compartments separated by a sintered-glass disk. The working macroelectrode was platinum gauze; a mercury pool was used as the counter electrode. The Amel potentiostat was connected to an Amel Model 558 integrator. Tests at low temperature were carried out with an Ag/AgCl reference electrode. All the potential values are referred to the SCE. Under the present experimental conditions, the ferrocenium/ferrocene couple was located at  $+0.49$  V.

ESR measurements were carried out with a Bruker ER 200-SRCB spectrometer operating at X-band ( $\omega_0 = 9.78$  GHz). The external magnetic field  $H_0$  was calibrated with a microwave bridge (Bruker ER 041 MR wave meter), and the temperature was controlled with a Bruker ER 4111 VT device (the accuracy was  $\pm 1$  °C).

**Reactions of  $[(\text{triphos})RhCl(C_2H_4)]$  with  $C_2H_2$ . A. At Reflux Temperature in THF.**  $[(\text{triphos})RhCl(C_2H_4)]$  (1.2 g, 1.5 mmol) was suspended in 30 mL of ethyne-saturated THF at room temperature, and the resulting mixture, maintained under an ethyne atmosphere, was rapidly brought to reflux temperature. The solid dissolved to give a red solution, and after 5 min brick red crystals of  $[(\text{triphos})Rh(\mu-Cl)(\mu-\eta^2, \eta^2-C_2H_2)Rh(\text{triphos})]Cl$  (**2**) began to form. Ethyne was replaced with nitrogen, the reaction mixture allowed to reach room temperature, and the precipitation completed by addition of *n*-heptane (5 mL). The crystals were collected by filtration and washed with *n*-pentane; yield 90%. Anal. Calcd for  $C_{84}H_{80}Cl_2P_6Rh_2$ : C, 65.00; H, 5.19; Rh, 13.26. Found: C, 64.92; H, 5.16; Rh, 13.11.  $\Delta_M = 76 \Omega^{-1} \text{ cm}^2 \text{ mol}^{-1}$ .

**B. At 0 °C in  $CH_2Cl_2$ .** Ethyne was bubbled through a solution of  $[(\text{triphos})RhCl(C_2H_4)]$  (1.2 g, 1.5 mmol) in  $CH_2Cl_2$  (100 mL) for 1 h at 0 °C. There was a gradual color change from orange to light red. Acetylene was replaced with nitrogen and after 15 min the solution warmed to room temperature. Acetone (50 mL) was added to the reaction mixture. On concentration to 10 mL off-white crystals of  $[(\text{triphos})RhCl(\eta^2-C_4H_4)]$  (**3**) as the acetone adduct began to form, the precipitation was completed by adding *n*-hexane (5 mL). They were filtered off and washed with *n*-pentane; yield 90%. Anal. Calcd for  $C_{48}H_{48}ClO_3P_3Rh$  (**3**· $(CH_3)_2CO$ ): C, 66.02; H, 5.66; Rh, 11.78. Found: C, 66.08; H, 5.59; Rh, 11.68.

**Metathetical Reaction of **2** with  $ClO_4^-$ ,  $PF_6^-$ , or  $BPh_4^-$ .** By recrystallization of **2** from  $CH_2Cl_2$ /ethanol mixtures in the presence of slight excesses of  $(NBu_4)ClO_4$ ,  $(NBu_4)PF_6$ ,  $TIPF_6$ , or  $NaBPh_4$  derivatives **2a**–**c** were obtained, respectively. Anal. Calcd for  $C_{84}H_{80}Cl_2O_4P_6Rh_2$  (**2a**): C, 62.43; H, 4.99; Rh, 12.73. Found: C, 62.12; H, 4.85; Rh, 12.45. Anal. Calcd for  $C_{84}H_{80}ClF_6P_7Rh_2$  (**2b**): C, 60.71; H, 4.85; Rh, 12.38. Found: C, 60.48; H, 4.85; Rh, 12.13.  $\Delta_M = 80 \Omega^{-1} \text{ cm}^2 \text{ mol}^{-1}$ . Anal. Calcd for  $C_{108}H_{100}BClF_6P_8Rh_2$  (**2c**): C, 70.66; H, 5.49; Rh, 11.21. Found: C, 70.53; H, 5.52; Rh, 11.13.

**Reaction of **2** with  $AgY$  ( $Y = ClO_4, PF_6, SO_3CF_3$ ).** A solution of the appropriate silver(I) salt (0.9 mmol) in acetone (20 mL) was added to a stirred solution of **2** (0.46 g, 0.3 mmol) in acetone (20 mL). After 2 h metallic silver and AgCl were eliminated by filtration and ethanol (30 mL) was added. When the solution stood overnight, brown-yellow crystals of  $[(\text{triphos})Rh(\mu-Cl)(\mu-OH)(\mu-\eta^1, \eta^1-C_2H_2)Rh(\text{triphos})]_2Y_2$  ( $Y = ClO_4$  (**4a**),  $PF_6$  (**4b**),  $SO_3CF_3$  (**4c**)) precipitated in ca. 85% yield. Anal. Calcd for  $C_{84}H_{81}Cl_3O_9P_6Rh_2$  (**4a**): C, 58.23; H, 4.71; Rh, 11.88. Found: C, 58.18; H, 4.69; Rh, 11.74. Anal. Calcd for  $C_{84}H_{81}ClF_{12}OP_8Rh_2$  (**4b**): C, 55.32; H, 4.47; Rh, 11.29. Found: C, 55.26; H, 4.46; Rh, 11.21.  $\Delta_M = 162 \Omega^{-1} \text{ cm}^2 \text{ mol}^{-1}$ . Anal. Calcd for  $C_{88}H_{81}ClF_6O_7P_6Rh_2S_2$  (**4c**):

(20) Smart, J. C.; Pinsky, B. L. *J. Am. Chem. Soc.* **1980**, *102*, 1009.

(21) Stephenson, D. S.; Binsch, G. *J. Magn. Reson.* **1980**, *37*, 395. Stephenson, D. S.; Binsch, G. *J. Magn. Reson.* **1980**, *37*, 409.



Table III. Summary of Crystal Data for 2c•DMF

formula	C <sub>111</sub> H <sub>107</sub> BCINOP <sub>6</sub> Rh <sub>2</sub>
fw	1908.86
cryst size	0.50 × 0.25 × 0.12
cryst syst	orthorhombic
space group	<i>Pccn</i> (No. 56)
<i>a</i> , Å	18.412 (3)
<i>b</i> , Å	19.823 (2)
<i>c</i> , Å	25.872 (5)
$\alpha$ , $\beta$ , $\gamma$ , deg	90.00
<i>V</i> , Å <sup>3</sup>	9442.78
<i>Z</i>	8
<i>d</i> (calcd), g cm <sup>-3</sup>	1.34
$\mu$ (Mo K $\alpha$ ), cm <sup>-1</sup>	5.21
radiation	graphite-monochromated Mo K $\alpha$ , $\lambda = 0.71069$ Å
scan type	$\omega$ - $2\theta$
$2\theta$ range, deg	5–45
scan width, deg	0.9 + 0.3 tan $\theta$
scan speed, deg s <sup>-1</sup>	0.03
total no. of data	6670
no. of unique data, $I \geq 3\sigma(I)$	2230
no. of params	179
<i>R</i>	0.063
<i>R<sub>w</sub></i>	0.068
abs cor min-max	0.817–1.099

C, 56.39; H, 4.46; Rh, 11.23. Found: C, 56.36; H, 4.41; Rh, 11.11.

**Reaction of 2a,b with AgY (Y = ClO<sub>4</sub>, PF<sub>6</sub>).** A solution of AgClO<sub>4</sub> (or AgPF<sub>6</sub>) (0.6 mmol) in acetone (20 mL) was added to a stirred solution of 2a (or 2b) (0.3 mmol) in acetone (20 mL). After 2 h metallic silver was eliminated by filtration and ethanol (30 mL) was added. When the solution stood overnight, brown-yellow crystals of 4a (or 4b) precipitated in ca. 85% yield.

**Reaction of 4a–c with HCl.** An excess of HCl dissolved in CH<sub>2</sub>Cl<sub>2</sub> (5 mL) was added to a CH<sub>2</sub>Cl<sub>2</sub> solution (20 mL) of 4a–c (0.25 mmol). Within a few minutes yellow crystals began to precipitate. Addition of ethanol (20 mL) completed the precipitation of [(triphos)Rh( $\mu$ -Cl)<sub>2</sub>( $\mu$ - $\eta^1$ -C<sub>2</sub>H<sub>2</sub>)Rh(triphos)]Y<sub>2</sub> (Y = ClO<sub>4</sub> (5a), PF<sub>6</sub> (5b), SO<sub>3</sub>CF<sub>3</sub> (5c)); yield ca. 90%. Anal. Calcd for C<sub>84</sub>H<sub>80</sub>Cl<sub>4</sub>O<sub>8</sub>P<sub>6</sub>Rh<sub>2</sub> (5a): C, 57.62; H, 4.60; Rh, 11.75. Found: C, 57.41; H, 4.51; Rh, 11.61. Anal. Calcd for C<sub>84</sub>H<sub>80</sub>Cl<sub>2</sub>F<sub>12</sub>P<sub>6</sub>Rh<sub>2</sub> (5b): C, 54.77; H, 4.38; Rh, 11.17. Found: C, 54.61; H, 4.41; Rh, 11.01.  $\Delta_M = 158 \Omega^{-1} \text{cm}^2 \text{mol}^{-1}$ . <sup>13</sup>C NMR (CD<sub>3</sub>NO<sub>2</sub>, 20 °C):  $\delta$ (C<sub>2</sub>H<sub>2</sub>) 162.4 ppm, <sup>1</sup>J(CRh) = 94.7 Hz, <sup>2</sup>J(CP<sub>trans</sub>) = 16.4 Hz, J(CH) = 164.0 Hz. Anal. Calcd for C<sub>86</sub>H<sub>80</sub>Cl<sub>2</sub>F<sub>6</sub>O<sub>6</sub>P<sub>6</sub>Rh<sub>2</sub>S<sub>2</sub> (5c): C, 55.83; H, 4.36; Rh, 11.12. Found: C, 55.79; H, 4.35; Rh, 10.99.

**Reaction of 2 with [(Cp)<sub>2</sub>Fe]PF<sub>6</sub>.** A solution of 2 (0.46 g, 0.3 mmol) in CH<sub>2</sub>Cl<sub>2</sub> (20 mL) was poured into a stirred CH<sub>2</sub>Cl<sub>2</sub> (20 mL) solution of [(Cp)<sub>2</sub>Fe]PF<sub>6</sub> (0.21 g, 0.65 mmol). Within a few minutes yellow crystals began to precipitate. Addition of ethanol (20 mL) completed the precipitation of 5b in 92% yield.

**Reaction of 4a with CF<sub>3</sub>COOH.** Neat CF<sub>3</sub>COOH (30  $\mu$ L, 0.38 mmol) was added to a CH<sub>2</sub>Cl<sub>2</sub> solution (30 mL) of 4a (0.25 g, 0.14 mmol). On addition of ethanol (20 mL) and concentration yellow crystals of [(triphos)Rh( $\mu$ -O<sub>2</sub>CCF<sub>3</sub>)( $\mu$ -Cl)( $\mu$ - $\eta^1$ -C<sub>2</sub>H<sub>2</sub>)Rh(triphos)](ClO<sub>4</sub>)<sub>2</sub> (6) precipitated in 90% yield. Anal. Calcd for C<sub>86</sub>H<sub>80</sub>Cl<sub>3</sub>F<sub>3</sub>O<sub>10</sub>P<sub>6</sub>Rh<sub>2</sub>: C, 56.49; H, 4.41; Rh, 11.25. Found: C, 56.51; H, 4.34; Rh, 11.14. <sup>13</sup>C NMR (CD<sub>3</sub>NO<sub>2</sub>, 20 °C):  $\delta$ (C<sub>2</sub>H<sub>2</sub>) 165.2 ppm, <sup>1</sup>J(CRh) = 92.8 Hz, <sup>2</sup>J(CP<sub>trans</sub>) = 17.2 Hz, <sup>1</sup>J(CH) = 163.0 Hz. IR:  $\nu$ (CF<sub>3</sub>) 1199 and 1147 cm<sup>-1</sup>.

**X-ray Data Collection and Structure Determination of 2c•DMF.** Crystals of compound 2c suitable for X-ray diffraction were obtained by crystallization from a DMF/1-butanol mixture, which gave 2c•DMF. A prismatic brick red crystal was mounted at random orientation on a glass fiber. An Enraf-Nonius CAD4 diffractometer was used both for the unit cell and space group determination and for data collection. Unit cell dimensions were obtained by a least-squares fit of the  $2\theta$  values of 25 high-order reflections ( $9.0 \leq \theta \leq 16.0^\circ$ ) with use of the CAD4 centering routines. Crystallographic and other relevant data collection parameters are listed in Table III. Data were measured with variable scan speed to ensure constant statistical precision on the collected intensities. As a general procedure, three standard reflections were collected every 2 h (no decay of intensities was observed in any case). Intensity data were corrected for Lorentz-polarization effects. Atomic scattering factors were those

Table IV. Final Positional Parameters ( $\times 10^4$ ) for 2c•DMF

atom	<i>x</i>	<i>y</i>	<i>z</i>
Rh1	2325 (1)	1683 (1)	807 (1)
P1	2167 (3)	994 (3)	1484 (2)
P2	1301 (3)	1153 (3)	426 (2)
P3	3108 (3)	868 (2)	430 (2)
Cl1	2500	2500	108 (2)
C1	2862 (8)	2429 (8)	1259 (5)
C2	1812 (11)	158 (9)	1273 (7)
C3	1514 (10)	250 (8)	335 (7)
C4	2844 (9)	19 (8)	625 (6)
C5	2016 (9)	-79 (8)	726 (6)
C6	1834 (11)	-846 (8)	714 (8)
C21	1773 (6)	1817 (6)	2295 (5)
C31	1309 (6)	2091 (6)	2666 (5)
C41	624 (6)	1809 (6)	2746 (5)
C51	402 (6)	1255 (6)	2454 (5)
C61	865 (6)	981 (6)	2083 (5)
C11	1551 (6)	1262 (6)	2003 (5)
C22	3642 (7)	1061 (6)	1799 (4)
C32	4225 (7)	889 (6)	2116 (4)
C42	4127 (7)	432 (6)	2520 (4)
C52	3444 (7)	148 (6)	2607 (4)
C62	2861 (7)	321 (6)	2290 (4)
C12	2959 (7)	777 (6)	1886 (4)
C23	280 (7)	1740 (6)	1076 (6)
C33	-367 (7)	1781 (6)	1355 (6)
C43	-854 (7)	1242 (6)	1351 (6)
C53	-693 (7)	661 (6)	1068 (6)
C63	-46 (7)	620 (6)	790 (6)
C13	441 (7)	1160 (6)	793 (6)
C24	4736 (7)	1515 (7)	4669 (5)
C34	4956 (7)	1648 (7)	4163 (5)
C41	4445 (7)	1657 (7)	3764 (5)
C54	3715 (7)	1532 (7)	3872 (5)
C64	3495 (7)	1400 (7)	4378 (5)
C14	4006 (7)	1391 (7)	4776 (5)
C25	2924 (7)	279 (5)	-569 (5)
C35	2971 (7)	288 (5)	-1108 (5)
C45	3277 (7)	842 (5)	-1359 (5)
C55	3537 (7)	1387 (5)	-1072 (5)
C65	3491 (7)	1378 (5)	-534 (5)
C15	3184 (7)	824 (5)	-283 (5)
C26	4494 (7)	316 (5)	607 (4)
C36	5242 (7)	358 (5)	686 (4)
C46	5576 (7)	987 (5)	730 (4)
C56	5161 (7)	1574 (5)	695 (4)
C66	4413 (7)	1532 (5)	616 (4)
C16	4079 (7)	903 (5)	572 (4)
B1	7500	2500	3170 (14)
C27	8459 (9)	1521 (7)	3327 (5)
C37	9015 (9)	1205 (7)	3601 (5)
C47	9225 (9)	1454 (7)	4083 (5)
C57	8878 (9)	2018 (7)	4290 (5)
C67	8321 (9)	2333 (7)	4016 (5)
C17	8112 (9)	2085 (7)	3534 (5)
C28	6411 (7)	1652 (7)	2979 (4)
C38	6060 (7)	1154 (7)	2692 (4)
C48	6355 (7)	939 (7)	2223 (4)
C58	7000 (7)	1222 (7)	2042 (4)
C68	7351 (7)	1720 (7)	2329 (4)
C18	7056 (7)	1936 (7)	2798 (4)
N1	7500	2500	575 (16)
C7	7468 (30)	1898 (25)	506 (20)
C8	7500	2500	1092 (21)
O1	7552 (19)	1487 (16)	608 (12)

reported by Cromer and Waber<sup>22</sup> with anomalous dispersion corrections taken from ref 23. All the calculations were done on a SEL 32/77 computer, installed in our institute, by using the SHELX 76 program.<sup>24</sup> The structure was solved by Patterson and Fourier techniques. Refinement was done by full-matrix least-squares calculations initially with isotopic thermal parameters.

(22) Cromer, D. T.; Waber, J. T. *Acta Crystallogr.* **1965**, *18*, 104.

(23) *International Tables for X-Ray Crystallography*; Kynoch Press: Birmingham, England, 1974; Vol. 4.

(24) Sheldrick, G. M. SHELX76 Program for Crystal Structure Determinations; University of Cambridge: Cambridge, England, 1976.

Anisotropic thermal parameters were used only for the Rh, P, and Cl atoms. The phenyl rings were treated as rigid bodies of  $D_{6h}$  symmetry with C-C distances fixed at 1.395 Å and calculated hydrogen atom positions (C-H = 0.96 Å). None of the residual peaks detected in the Fourier difference map allowed us to localize the ethyne hydrogen atoms. Atomic coordinates for all the non-hydrogen atoms are given in Table IV.

**Acknowledgment.** This work was supported by "Progetto Finalizzato Chimica Fine e Secondaria", CNR,

Rome, Italy.

**Supplementary Material Available:** Final positional parameters for hydrogen atoms (Table V) and refined anisotropic and isotropic temperature factors (Table VI) for **2c**-DMF, the cyclic voltammogram behavior of **2b** in  $\text{CH}_2\text{Cl}_2$  (Figure 8), and the cyclic voltammogram of **2b** in  $\text{CH}_2\text{Cl}_2$  after exhaustive two-electron oxidation (Figure 9) (5 pages); a listing of observed and calculated structure factors for **2c**-DMF (13 pages). Ordering information is given on any current masthead page.

## Coupling of Two Ethyne Molecules at Rhodium versus Coupling of Two Rhodium Atoms at Ethyne. 2. Implications for the Reactivity. Catalytic and Stoichiometric Functionalization Reactions of Ethyne

Claudio Bianchini,\* Andrea Meli, Maurizio Peruzzini, Alberto Vacca, and Francesco Vizza

*Istituto per lo Studio della Stereochimica ed Energetica dei Composti di Coordinazione, CNR,  
Via J. Nardi 39, 50132 Firenze, Italy*

Received May 16, 1990

The rhodacyclopentadiene complex  $[(\text{triphos})\text{RhCl}(\eta^2\text{-C}_4\text{H}_4)]$  (**3**) has been synthesized by treatment of  $[(\text{triphos})\text{RhCl}(\text{C}_2\text{H}_2)]$  (**1**) in  $\text{CH}_2\text{Cl}_2$  with an excess of ethyne (triphos =  $\text{MeC}(\text{CH}_2\text{PPh}_2)_3$ ). Complex **3** catalyzes under very mild conditions the cyclotrimerization of ethyne to benzene as well as the cyclo-oligomerization of ethyne with acetonitrile to 2-picoline. A plausible catalysis cycle for both reactions is proposed on the basis of multiform experimental evidence. Complex **3** is a potential synthon for the preparation of a variety of heterocyclic compounds containing the  $\text{C}_4\text{H}_4$  diene moiety. As an example, **3** reacts with dimethyl acetylenedicarboxylate, carbon disulfide, and *cyclo*-octasulfur, producing dimethyl phthalate, dithiopyrone, and thiophene, respectively. Carbon monoxide reacts with **3** in the presence of  $\text{TIPF}_6$ , yielding  $[(\text{triphos})\text{Rh}(\eta^4\text{-C}_4\text{H}_4\text{CO})]\text{PF}_6$  (**10**), which contains an unsubstituted cyclopentadienone ligand. By treatment with  $\text{H}_2$ , **3** transforms into the  $\eta^4$ -butadiene derivative  $[(\text{triphos})\text{Rh}(\eta^4\text{-C}_4\text{H}_6)]\text{BPh}_4$  (**13**). The chemistry of **3** has been compared to and contrasted with that of the related *perpendicular*  $\mu\text{-C}_2\text{H}_2$  complex  $[(\text{triphos})\text{Rh}(\mu\text{-Cl})(\mu\text{-}\eta^2, \eta^2\text{-C}_2\text{H}_2)\text{Rh}(\text{triphos})]\text{Cl}$  (**2**). From this study it is concluded that coupling of two or more metal centers at acetylene may lead to inactive complexes for catalytic transformations of acetylene.

### Introduction

In the preceding article,<sup>1</sup> we have shown that the reaction between  $[(\text{triphos})\text{RhCl}(\text{C}_2\text{H}_2)]^2$  (**1**) and ethyne can selectively give either the bridging  $\text{C}_2\text{H}_2$  dimer  $[(\text{triphos})\text{Rh}(\mu\text{-Cl})(\mu\text{-}\eta^2, \eta^2\text{-C}_2\text{H}_2)\text{Rh}(\text{triphos})]\text{Cl}$  (**2**) or the product originated by coupling of two ethyne molecules at the metal, the rhodacyclopentadiene  $[(\text{triphos})\text{RhCl}(\eta^2\text{-C}_4\text{H}_4)]$  (**3**) (triphos =  $\text{MeC}(\text{CH}_2\text{PPh}_2)_3$ ) (Scheme I). Along with a detailed characterization of the rhodacyclopentadiene complex, in this paper we compare and contrast the reactions of **2** and **3** with a variety of selected reagents. The two complexes exhibit quite different chemical properties. Distinct reactivities for **2** and **3** are not surprising and could well be predicted in view of their different structures. However, the question is not of trivial importance, since the two compounds form from the same reaction and only a subtle change of the conditions tips the balance in favor of either product.

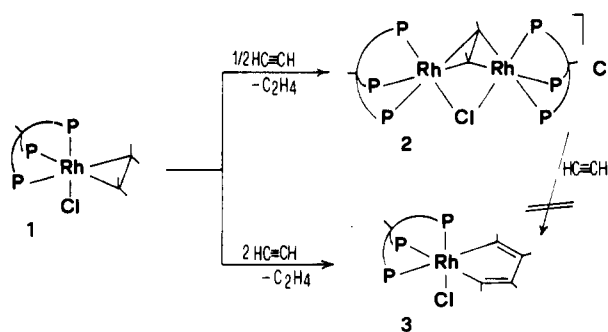
### Results and Discussion

As anticipated in the preceding article,<sup>1</sup> the most convenient way to synthesize the rhodacyclopentadiene com-

(1) Bianchini, C.; Masi, D.; Meli, A.; Peruzzini, M.; Vacca, A.; Laschi, F.; Zanella, P. *Organometallics*, preceding paper in this issue.

(2) Bianchini, C.; Meli, A.; Peruzzini, M.; Vizza, F.; Frediani, P.; Ramirez, J. A. *Organometallics* 1990, 9, 226.

Scheme I



plex **3** is to dissolve **1** in dichloromethane previously saturated with ethyne at 0 °C. Addition of a mixture of acetone/*n*-hexane precipitates  $3 \cdot (\text{CH}_3)_2\text{CO}$  as off-white crystals, which are stable in the solid state and in deoxygenated solutions. The complex behaves as a nonelectrolyte in  $\text{CH}_2\text{Cl}_2$  and  $\text{EtNO}_2$ , where it is monomeric as determined by molecular weight measurements. The IR spectrum contains a weak band at  $1495 \text{ cm}^{-1}$ , which can be assigned to  $\nu(\text{C}=\text{C})$  within the metallacycle.<sup>3</sup>

(3) Alt, H. G.; Engelhardt, H. E.; Rausch, M. D.; Kool, L. B. *J. Organomet. Chem.* 1987, 329, 61.